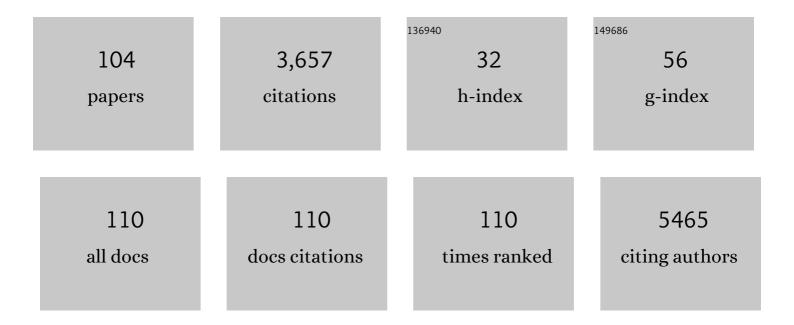
## Patrizia Canton

List of Publications by Year in descending order

Source: https://exaly.com/author-pdf/7949234/publications.pdf Version: 2024-02-01



#	Article	IF	CITATIONS
1	Selective oxidation of glycerol with oxygen using mono and bimetallic catalysts based on Au, Pd and Pt metals. Catalysis Today, 2005, 102-103, 203-212.	4.4	304
2	Double rare-earth nanothermometer in aqueous media: opening the third optical transparency window to temperature sensing. Nanoscale, 2017, 9, 3079-3085.	5.6	145
3	Effects of gold nanoparticles deposition on the photocatalytic activity of titanium dioxide under visible light. Physical Chemistry Chemical Physics, 2009, 11, 7171.	2.8	126
4	Clusters of Poly(acrylates) and Silver Nanoparticles: Structure and Applications for Antimicrobial Fabrics. Journal of Physical Chemistry C, 2008, 112, 11758-11766.	3.1	122
5	Consecutive hydrogenation of benzaldehyde over Pd catalysts. Applied Catalysis A: General, 2001, 219, 195-200.	4.3	109
6	Influence of Particle Size and Crystal Orientation on the Electrochemical Behavior of Carbon-Coated LiFePO <sub>4</sub> . Journal of Physical Chemistry C, 2010, 114, 12598-12603.	3.1	108
7	Nucleation and crystallization behavior of glass-ceramic materials in the Li2O–Al2O3–SiO2 system of interest for their transparency properties. Journal of Non-Crystalline Solids, 2001, 288, 127-139.	3.1	106
8	A Versatile Approach to the Synthesis of Functionalized Thiol-Protected Palladium Nanoparticles. Chemistry of Materials, 2011, 23, 3961-3969.	6.7	94
9	Pd/CO Average Chemisorption Stoichiometry in Highly Dispersed Supported Pd/γ-Al2O3Catalysts. Langmuir, 2002, 18, 6530-6535.	3.5	93
10	Generation of Size-Controlled PdO Nanoclusters inside Nanoporous Domains of Gel-Type Resins: Diverse and Convergent Evidence That Supports a Strategy of Template-Controlled Synthesis. Angewandte Chemie - International Edition, 2004, 43, 959-962.	13.8	92
11	Calcium hydroxide nanoparticles from solvothermal reaction for the deacidification of degraded waterlogged wood. Journal of Colloid and Interface Science, 2016, 473, 1-8.	9.4	81
12	Gold Nanoparticles Incarcerated in Nanoporous Syndiotactic Polystyrene Matrices as New and Efficient Catalysts for Alcohol Oxidations. Chemistry - A European Journal, 2012, 18, 709-715.	3.3	71
13	Hydrogen production through alcohol steam reforming on Cu/ZnO-based catalysts. Applied Catalysis B: Environmental, 2011, 101, 397-408.	20.2	69
14	Pd-Fe/SiO2 Catalysts in the Hydrogenation of 2,4-Dinitrotoluene. Journal of Catalysis, 1994, 150, 356-367.	6.2	64
15	Highly efficient and selective reduction of nitroarenes into anilines catalyzed by gold nanoparticles incarcerated in a nanoporous polymer matrix: Role of the polymeric support and insight into the reaction mechanism. Journal of Catalysis, 2016, 340, 30-40.	6.2	64
16	Nanostructural Features of Pd/C Catalysts Investigated by Physical Methods:Â A Reference for Chemisorption Analysis. Langmuir, 2000, 16, 4539-4546.	3.5	63
17	Upconverting Nanoparticle to Quantum Dot Förster Resonance Energy Transfer: Increasing the Efficiency through Donor Design. ACS Photonics, 2018, 5, 2261-2270.	6.6	63
18	Alumina-Promoted Sulfated Zirconia System:Â Structure and Microstructure Characterization. Chemistry of Materials, 2001, 13, 1634-1641.	6.7	57

#	Article	IF	CITATIONS
19	Wustite as a new precursor of industrial ammonia synthesis catalysts. Applied Catalysis A: General, 2003, 251, 121-129.	4.3	53
20	Formation and Controlled Growth of Bismuth Titanate Phases into Mesoporous Silica Nanoparticles: An Efficient Self-Sealing Nanosystem for UV Filtering in Cosmetic Formulation. ACS Applied Materials & Interfaces, 2017, 9, 1913-1921.	8.0	53
21	Quantitative Phase Analysis in Semicrystalline Materials Using the Rietveld Method. Journal of Applied Crystallography, 1998, 31, 78-82.	4.5	52
22	Optimization of bimetallic dry reforming catalysts by temperature programmed reaction. Applied Catalysis A: General, 2012, 439-440, 80-87.	4.3	52
23	Luminescence of Eu3+ Activated CaF2 and SrF2 Nanoparticles: Effect of the Particle Size and Codoping with Alkaline Ions. Crystal Growth and Design, 2018, 18, 686-694.	3.0	52
24	Pd-Au and Pd-Pt catalysts for the direct synthesis of hydrogen peroxide in absence of selectivity enhancers. Applied Catalysis A: General, 2013, 468, 160-174.	4.3	47
25	TiO <sub>2</sub> –mesoporous silica nanocomposites: cooperative effect in the photocatalytic degradation of dyes and drugs. RSC Advances, 2014, 4, 37826-37837.	3.6	47
26	Effect of the matrix in niobium-based aerogel catalysts for the selective oxidation of olefins with hydrogen peroxide. Journal of Catalysis, 2005, 229, 490-498.	6.2	44
27	X-ray Rietveld Analysis with a Physically Based Background. Journal of Applied Crystallography, 1995, 28, 115-120.	4.5	43
28	Nd3+ activated CaF2 NPs as colloidal nanothermometers in the biological window. Optical Materials, 2017, 68, 29-34.	3.6	42
29	Synthesis and catalytic activity of metal nanoclusters inside functional resins: an endeavour lasting 15 years. Philosophical Transactions Series A, Mathematical, Physical, and Engineering Sciences, 2010, 368, 1495-1507.	3.4	41
30	ASAXS study of Au, Pd and Pd–Au catalysts supported on active carbon. Catalysis Today, 1999, 49, 485-489.	4.4	35
31	Field-assisted ion diffusion of transition metals for the synthesis of nanocomposite silicate glasses. Materials Science and Engineering C, 2006, 26, 1087-1091.	7.3	33
32	Magnetic nanoparticle clusters as actuators of ssDNA release. Physical Chemistry Chemical Physics, 2014, 16, 10023.	2.8	33
33	Covering the optical spectrum through collective rare-earth doping of NaGdF <sub>4</sub> nanoparticles: 806 and 980 nm excitation routes. Physical Chemistry Chemical Physics, 2017, 19, 11825-11834.	2.8	33
34	Synthesis of novel allyl palladium complexes bearing purine based NHC and a water soluble phosphine and their catalytic activity in the Suzukiâ€Miyaura coupling in water. Applied Organometallic Chemistry, 2018, 32, e4034.	3.5	33
35	Bi <sub>2</sub> SiO <sub>5</sub> @g-SiO <sub>2</sub> upconverting nanoparticles: a bismuth-driven core–shell self-assembly mechanism. Nanoscale, 2019, 11, 675-687.	5.6	31
36	Nanocrystalline alanates—Phase transformations, and catalysts. Journal of Alloys and Compounds, 2005, 404-406, 732-737.	5.5	30

#	Article	IF	CITATIONS
37	Bimetallic Pd–Au catalysts for benzaldehyde hydrogenation: Effects of preparation and of sulfur poisoning. Catalysis Communications, 2008, 9, 2353-2356.	3.3	30
38	Chemoselective and re-usable heterogeneous catalysts for the direct synthesis of hydrogen peroxide in the liquid phase under non-explosive conditions and in the absence of chemoselectivity enhancers. Applied Catalysis A: General, 2009, 358, 224-231.	4.3	30
39	The effect of Al2O3-promotion of sulfated zirconia on n-butane isomerization: An isotopic transient kinetic analysis. Catalysis Communications, 2006, 7, 209-213.	3.3	29
40	Synchrotron X-Ray Studies of Ti-Doped NaAlH4. Journal of Physical Chemistry B, 2006, 110, 3051-3054.	2.6	29
41	Polymorphism and magnetic properties of Li2MSiO4 (M = Fe, Mn) cathode materials. Scientific Reports, 2013, 3, 3452.	3.3	29
42	Mesoporous silica nanoparticles with tunable pore size for tailored gold nanoparticles. Journal of Nanoparticle Research, 2014, 16, 1.	1.9	29
43	Au/C Catalyst:  Experimental Evidence of the Coexistence of Nanoclusters and Larger Au Particles. Langmuir, 1998, 14, 6617-6619.	3.5	27
44	Colloidal nanothermometers based on neodymium doped alkaline-earth fluorides in the first and second biological windows. Sensors and Actuators B: Chemical, 2017, 250, 147-155.	7.8	27
45	Structure and Size of Poly-Domain Pd Nanoparticles Supported on Silica. Catalysis Letters, 2003, 88, 141-146.	2.6	26
46	Selective Hydrogenations and Dechlorinations in Water Mediated by Anionic Surfactant-Stabilized Pd Nanoparticles. Journal of Organic Chemistry, 2018, 83, 7438-7446.	3.2	26
47	Mercaptosilane-Passivated CulnS2 Quantum Dots for Luminescence Thermometry and Luminescent Labels. ACS Applied Nano Materials, 2019, 2, 2426-2436.	5.0	26
48	Calibration of the monochromator bandpass function for the X-ray Rietveld analysis. Powder Diffraction, 1997, 12, 160-166.	0.2	24
49	Laser beam irradiation of silver doped silicate glasses. Nuclear Instruments & Methods in Physics Research B, 2010, 268, 3177-3182.	1.4	24
50	Increasing the Antibacterial Effect of Lysozyme by Immobilization on Multi-Walled Carbon Nanotubes. Journal of Nanoscience and Nanotechnology, 2011, 11, 3100-3106.	0.9	24
51	Gel-type ion exchange resin stabilized Pd-Bi nanoparticles for the glycerol oxidation in liquid phase. Journal of Industrial and Engineering Chemistry, 2016, 39, 77-86.	5.8	24
52	Bismuth titanate-based UV filters embedded mesoporous silica nanoparticles: Role of bismuth concentration in the self-sealing process. Journal of Colloid and Interface Science, 2019, 549, 1-8.	9.4	24
53	Patterned nanoporous-gold thin layers: Structure control and tailoring of plasmonic properties. Microporous and Mesoporous Materials, 2012, 163, 153-159.	4.4	23
54	Determining the Degree of Crystallinity in Semicrystalline Materials by means of the Rietveld Analysis. Journal of Applied Crystallography, 1995, 28, 121-126.	4.5	22

#	Article	IF	CITATIONS
55	Thermal Evolution of Carbon-Supported Pd Nanoparticles Studied by Time-Resolved X-ray Diffraction. Journal of Physical Chemistry B, 2001, 105, 8088-8091.	2.6	22
56	Microgel electrospinning: A novel tool for the fabrication of nanocomposite fibers. Polymer, 2009, 50, 6193-6197.	3.8	21
57	TiO2 nanoparticles obtained by laser ablation in water: Influence of pulse energy and duration on the crystalline phase. Journal of Alloys and Compounds, 2015, 643, S75-S79.	5.5	20
58	TEM and XRD investigation of Pd on ultradispersed diamond, correlation with catalytic activity. Mendeleev Communications, 2009, 19, 133-135.	1.6	19
59	Engineering efficient upconverting nanothermometers using Eu3+ ions. Nanoscale Advances, 2019, 1, 757-764.	4.6	19
60	Structural and physical properties of cobalt nanocluster composite glasses. Journal of Non-Crystalline Solids, 2004, 336, 148-152.	3.1	18
61	WO3/ZrO2 catalysts by sol–gel processing. Journal of Non-Crystalline Solids, 1998, 225, 178-183.	3.1	17
62	Fluorinated and Charged Hydrogenated Alkanethiolates Grafted on Gold: Expanding the Diversity of Mixed-Monolayer Nanoparticles for Biological Applications. Bioconjugate Chemistry, 2017, 28, 43-52.	3.6	17
63	Triphasic liquid systems: generation and segregation of catalytically active Pd nanoparticles in an ammonium-based catalyst-philic phase. Chemical Communications, 2006, , 4480.	4.1	16
64	Template controlled synthesis of monometallic zerovalent metal nanoclusters inside cross-linked polymer frameworks: the effect of a single matrix on the size of different metal nanoparticles. New Journal of Chemistry, 2010, 34, 2956.	2.8	16
65	Bottom-up/top-down synthesis of stable zirconium hydroxide nanophases. Journal of Materials Chemistry, 2012, 22, 23497.	6.7	16
66	Some structural and optical properties of copper and copper oxide nanoparticles in silica films formed by co-deposition of copper and silica. Journal of Non-Crystalline Solids, 2005, 351, 1932-1936.	3.1	15
67	Size dependent hcp-to-fcc transition temperature in Co nanoclusters obtained by ion implantation in silica. Nuclear Instruments & Methods in Physics Research B, 2006, 250, 206-209.	1.4	15
68	Cross-linked poly-vinyl polymers versus polyureas as designed supports for catalytically active M0 nanoclusters. Journal of Molecular Catalysis A, 2009, 300, 48-58.	4.8	15
69	Cross-linked polyvinyl polymers versus polyureas as designed supports for catalytically active M0 nanoclusters : Part III. Nanometer scale structure of the cross-linked polyurea support EnCat 30 and of the PdII/EnCat 30 and Pd0/EnCat 30NP catalysts. Physical Chemistry Chemical Physics, 2009, 11, 4068.	2.8	15
70	Cu/Ag-based bifunctional nanoparticles obtained by one-pot laser-assisted galvanic replacement. Journal of Nanoparticle Research, 2013, 15, 1.	1.9	15
71	Characterization of Nanoporous Lanthanide-Doped Gadolinium Gallium Garnet Powders Obtained by Propellant Synthesis. Materials Science Forum, 2005, 494, 143-148.	0.3	14
72	A tri-block copolymer templated synthesis of gold nanostructures. Journal of Colloid and Interface Science, 2011, 357, 88-94.	9.4	14

#	Article	IF	CITATIONS
73	Surfactantâ€Induced Substrate Selectivity in the Palladiumâ€Nanoparticleâ€Mediated Chemoselective Hydrogenation of Unsaturated Aldehydes in Water. ChemCatChem, 2014, 6, 1575-1578.	3.7	14
74	Novel nanostructured semicrystalline ionomers by chemoselective sulfonation of multiblock copolymers of syndiotactic polystyrene with polybutadiene. RSC Advances, 2014, 4, 60158-60167.	3.6	14
75	Rietveld analysis of the cubic crystal structure of Na-stabilized zirconia. Journal of Materials Research, 1997, 12, 318-321.	2.6	13
76	Scale Factor in Powder Diffraction. Acta Crystallographica Section A: Foundations and Advances, 1998, 54, 219-224.	0.3	13
77	Detecting palladium nanoparticles in Pd/C catalysts using Xâ€ray Rietveld method. Catalysis Letters, 2000, 64, 119-124.	2.6	13
78	Gel-Type Cross-Linked Functional Polymers as Template in the Synthesis of Size Controlled Metal Nanoclusters. , 2008, , 413-418.		13
79	Gold stabilized aqueous sols immobilized on mesoporous CeO2–Al2O3 as catalysts for the preferential oxidation of carbon monoxide. Journal of Colloid and Interface Science, 2010, 350, 435-442.	9.4	12
80	Stabilization of cubic Na-modified ZrO2: a neutron diffraction study. Journal of Applied Crystallography, 1999, 32, 475-480.	4.5	11
81	Neutron diffraction study of mechanically alloyed and in situ annealed Al75Mo25 powders. Journal of Applied Physics, 2000, 87, 2753-2759.	2.5	11
82	Highly Hydrophilic Copolymers of <i>N</i> , <i>N</i> â€Dimethylacrylamide, Acrylamidoâ€2â€methylpropanesulfonic acid, and Ethylenedimethacrylate: Nanoscale Morphology in the Swollen State and Use as Exotemplates for Synthesis of Nanostructured Ferric Oxide. Chemistry - A European Journal, 2012, 18, 6632-6643.	3.3	11
83	SERS and catalytically active Ag/Pd nanoparticles obtained by combining laser ablation and galvanic replacement. Journal of Alloys and Compounds, 2014, 615, S352-S356.	5.5	11
84	Radiofrequency magnetron co-sputtering deposition synthesis of Co-based nanocomposite glasses for optical and magnetic applications. Applied Surface Science, 2004, 226, 62-67.	6.1	10
85	Biphase hydroformylation catalyzed by rhodium in combination with a water-soluble pyridyl-triazole ligand. Inorganica Chimica Acta, 2017, 455, 613-617.	2.4	10
86	A semi-empirical asymmetry function for X-ray diffraction peak profiles. Powder Diffraction, 1995, 10, 204-206.	0.2	9
87	Influence of preparation procedure on physical and catalytic properties of carbon supported Pd-Au catalysts Studies in Surface Science and Catalysis, 2000, 143, 1011-1018.	1.5	9
88	Thermal evolution of cobalt nanocrystals embedded in silica. Materials Science and Engineering C, 2007, 27, 193-196.	7.3	9
89	The metathesis of $\hat{l}_{\pm}$ -olefins over supported Re-catalysts in supercritical CO <sub>2</sub> . Green Chemistry, 2009, 11, 229-238.	9.0	9
90	Synthesis of Nanocomposites from Pd <sup>0</sup> and a Hyperâ€Crossâ€Linked Functional Resin Obtained from a Conventional Gelâ€Type Precursor. Chemistry - A European Journal, 2013, 19, 9381-9387.	3.3	9

#	Article	IF	CITATIONS
91	Influence of Metal Precursors and Reduction Protocols on the Chlorideâ€Free Preparation of Catalysts for the Direct Synthesis of Hydrogen Peroxide without Selectivity Enhancers. ChemCatChem, 2016, 8, 1564-1574.	3.7	9
92	A study of Al-Mo alloys synthetized by mechanical treatment and annealed in-situ. Scripta Materialia, 1999, 12, 547-550.	0.5	8
93	Nanoscale Characterization of Metal Nanoclusters by Means of X-Ray Diffraction (XRD) and Transmission Electron Microscopy (TEM) Techniques. , 2008, , 129-147.		8
94	Metal catalysis with nanostructured metals supported on strongly acidic cross-linked polymer frameworks. Part I. The behaviour of M2+ ions (M=Ni, Pd, Pt, Cu) supported on Rohm & Haas's resin A70 and Du Pont's SAC-13, towards H2 in the solid state and NaBH4 in aqueous medium. Reactive and Functional Polymers, 2010, 70, 639-646.	4.1	8
95	Copper-based nanocluster composite silica films by rf-sputtering deposition. Materials Science and Engineering C, 2006, 26, 1092-1096.	7.3	7
96	In situ wide angle X-ray scattering (WAXS) study of bimetallic Au–Pd catalysts. Catalysis Letters, 2000, 69, 17-20.	2.6	6
97	Influence of halide ions on the structure and properties of copper indium sulphide quantum dots. Chemical Communications, 2020, 56, 3341-3344.	4.1	6
98	Metal catalysis with nanostructured metals supported inside strongly acidic cross-linked polymer frameworks: Influence of reduction conditions of AullI-containing resins on metal nanoclusters formation in macroreticular and gel-type materials. Inorganica Chimica Acta, 2012, 391, 114-120.	2.4	5
99	Metal nanoclusters stabilized by pH-responsive microgels: Preparation and evaluation of their catalytic potential. Reactive and Functional Polymers, 2017, 115, 81-86.	4.1	5
100	Seeded growth of gold nanorods: the effect of sulfur-containing quenching agents. Journal of Nanoparticle Research, 2018, 20, 1.	1.9	4
101	Resonant-XRD Characterization of Nanoalloyed Au-Pd Catalysts for the Direct Synthesis of H2O2: Quantitative Analysis of Size Dependent Composition of the Nanoparticles â€. Applied Sciences (Switzerland), 2019, 9, 2959.	2.5	4
102	Microgels as Soluble Scaffolds for the Preparation of Noble Metal Nanoparticles Supported on Nanostructured Metal Oxides. ACS Applied Nano Materials, 2021, 4, 8343-8351.	5.0	4
103	Polymer-Hematite Nanocomposites: Templating Effect of Commercial Ion-Exchangers in the Growth of Size-Controlled Iron Oxide Nanoparticles. Journal of Nanoscience and Nanotechnology, 2013, 13, 6872-6879.	0.9	2
104	Ionic liquid mediated deposition of ruthenium mirrors on glass under multiphase conditions. New Journal of Chemistry, 2016, 40, 1948-1952.	2.8	1